JACS
JOURNAL OF THE AMERICAN CHEMICAL SOCIETY
Communication
pubs.acs.org/JACS

Synthesis of Ultralong Copper Nanowires for High-Performance Transparent Electrodes

Dieqing Zhang,[†,⊥] Ranran Wang,[‡,∥,⊥] Meicheng Wen,[†] Ding Weng,[∥] Xia Cui,[§,∥] Jing Sun,*[,‡] Hexing Li,*[,†] and Yunfeng Lu*[,∥]

[†]Key Laboratory of Resource Chemistry of the Ministry of Education, Shanghai Normal University, Shanghai 200234, China

[‡]State Key Laboratory of High Performance Ceramics and Superfine Microstructure, Shanghai Institute of Ceramics, Chinese Academy of Sciences, Shanghai 200050, China

[§]Department of Chemistry and Chemical Engineering, Southeast University, Nanjing 211189, China

[∥]Department of Chemical and Biomolecular Engineering, University of California, Los Angeles, California 90095, United States

Supporting Information

ABSTRACT: Cu nanowires hold great promise for the fabrication of low-cost transparent electrodes. However, their current synthesis is mainly performed in aqueous media with poor nanowire dispersibility. We report herein the novel synthesis of ultralong single-crystalline Cu nanowires with excellent dispersibility, providing an excellent candidate material for high-performance transparent electrode fabrication.

Transparent electrodes are essential for the fabrication of flat-panel displays, touch screens, organic light-emitting diodes, solar cells, and other electronic devices. Traditionally, such electrodes are based on indium tin oxide (ITO), the price of which has increased nearly 10-fold in the past decade.[1] The search for low-cost alternatives has attracted much attention. In this context, thin films of carbon nanotubes (CNTs),[2] graphene,[3] and metal nanowires[4] have been explored extensively. While thin films of CNTs and graphene exhibit promising performance, their sheet resistances (100−1000 Ω/□ at 80−90% optical transmittance)[5] are still high for most applications. Thin films of metal nanowires, in comparison, hold great promise because of their high conductivity and optical transmittance. For example, thin films of Ag nanowires have been shown to exhibit conductivities and transmittance comparable to those of ITO.[6] Compared with Ag, Cu is 1000 times more abundant and 100 times less expensive. Developing Cu-based thin films has therefore emerged as a highly promising approach leading toward low-cost transparent electrodes.

To date, Cu nanowire electrodes have mainly been fabricated using two different approaches. The first approach is based on the electrospinning process,[7] in which nanofibers of poly(vinyl alcohol) containing copper acetate are spun onto glass substrates. Subsequent calcination followed by hydrogen reduction leads to the formation of Cu nanofiber networks with excellent conductivity and optical transmittance (~50 Ω/□ at ~90% transmittance). However, this method requires high processing temperatures (e.g., ~500 °C) and has limited applicability. The other approach is based on Cu nanowire inks, where transparent electrodes are fabricated by spray- or rod-coating the nanowire ink on the substrate.[4,8] Large-scale fabrication of transparent electrodes could be achieved using this approach if high-quality Cu nanowires could be synthesized effectively.

In the context of Cu nanowire synthesis, the current techniques mainly rely on aqueous-media reduction of Cu salts. For example, Cu nanowires with an average diameter of ~90 nm and length of ~10 μm were synthesized by hydrazine reduction of $Cu(NO_3)_2$.[1] However, this synthesis led to nanowires with poor dispersibility and a significant amount of Cu particles, which could deteriorate the electrode performance dramatically. Recently, Cu nanowires with a smaller diameter (~24 nm) and lengths of up to hundreds of micrometers were synthesized by glucose reduction of $CuCl_2$ in the presence of hexadecylamine (HDA).[9] However, similar to the former approach, these nanowires also tended to aggregate, forming large-sized bundles. In addition, these long nanowires exhibited the pentatwinned crystalline structure, which is less conductive[10] and easier to oxidize than those with a single-crystal structure.[11]

Herein, we report a nonaqueous synthesis of ultralong single-crystalline Cu nanowires with excellent dispersibility. Our synthesis strategy relies on self-catalytic growth of Cu nanowires within a liquid-crystalline medium of HDA and cetyltriamonium bromide (CTAB). HDA and CTAB are first mixed at elevated temperature to form a liquid-crystalline medium. Upon addition of the precursor, copper acetylacetonate [$Cu(acac)_2$], ultralong nanowires with excellent dispersibility form spontaneously within the medium in the presence of a catalytic Pt surface.

Figure 1a shows scanning electron microscopy (SEM) images of the nanowires. The average diameter of the nanowires was ~78 nm, as calculated from 50 nanowires randomly selected from the SEM images. The lengths of the nanowires varied from tens to hundreds of micrometers; some of them were as long as several millimeters. Unlike the bundled nanowires mentioned above, these nanowires were well-dispersed, as shown by both SEM and transmission electron microscopy (TEM) images. The magnified SEM image (Figure 1a inset) discloses that the nanowires exhibited a hexagonal cross section. On the basis of selected-area electron diffraction (SAED) analysis (Figure 1c), these nanowires were consistently found to be single-crystalline,

Received: May 23, 2012
Published: July 19, 2012

dx.doi.org/10.1021/ja3050184 | J. Am. Chem. Soc. 2012, 134, 14283−14286

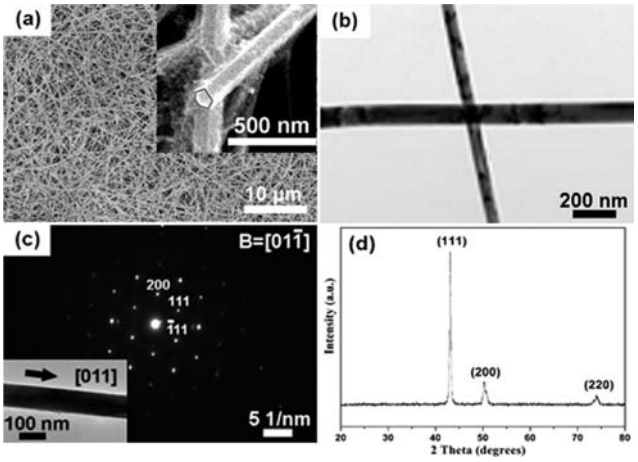

Figure 1. (a) SEM and (b) TEM images of Cu nanowires. (c) SAED pattern of the Cu nanowire shown in the inset. (d) XRD pattern of Cu nanowires.

growing along the [011] direction. Figure 1d shows the X-ray diffraction (XRD) pattern of the nanowires. The peaks at 2θ = 43.2, 50.3, and 74.1° correspond to the diffractions from the {220} planes of face-centered cubic (fcc) Cu (JCPDS card no. 03-1018). No other peaks were observed, indicating the pure-phase nature of the nanowires.

The structure of the nanowires was further studied by high-resolution TEM (HRTEM). On the basis of the above analysis, these nanowires were single-crystalline and grew along the [011] direction. Consistent with such a growth direction, the side faces of the nanowires should be the ±(200), ±(1$\bar{1}$1), and ±(11$\bar{1}$) planes. This conjecture was confirmed by the HRTEM images of two different nanowires (Figure 2c,d), which clearly showed

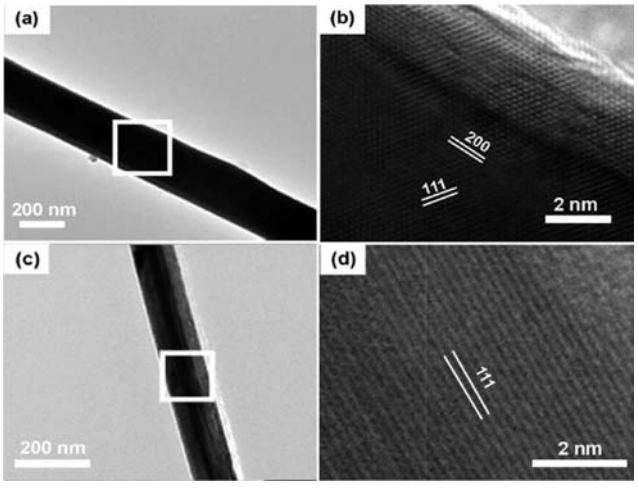

Figure 2. (a, c) TEM images of two different Cu nanowires. (b, d) HRTEM images of the boxed areas in (a) and (c), respectively.

fringes corresponding to the {200} and {111} planes along the axis of the nanowires. The angle between the {111} planes and that between the {200} and {111} planes were 109.5° and 125.3°, respectively, consistent with the proposed crystal structure. Although various morphologies of metal nanowires and nanorods have been reported, such as rectangular wires, octagonal wires, right-bipyramidal beams, and pentagonal wires,[11] to the best of our knowledge, it is the first report of hexagonal metal nanowires. The successful synthesis of hexagonal Cu nanowires enriches the morphological control of metal nanowires, sheding light on the shape control of metal crystals.

In an effort to uncover the growth mechanism, the structural evolution of the nanowires was probed. An SEM image recorded after 2 h of reaction exhibited the presence of Cu nanocrystals and nanowires, and the development of nanowire embryos from the nanoparticles was also observed (Figure 3a). One question is

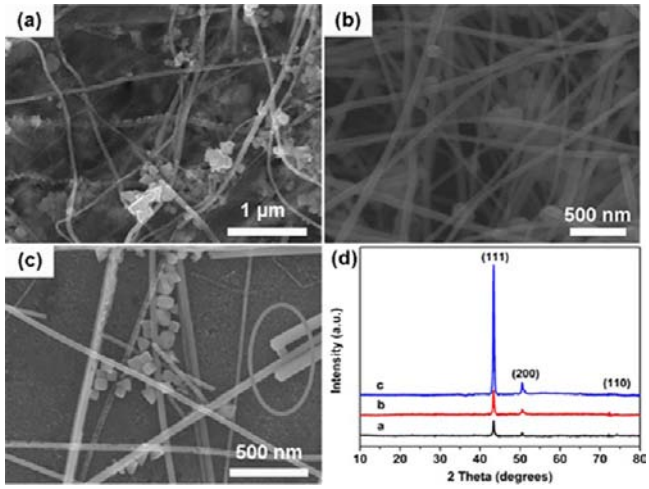

Figure 3. (a–c) SEM images of Cu nanowires synthesized at reaction times of (a) 2, (b) 5, and (c) 10 h. (d) XRD patterns of the Cu nanowires in (a–c).

the following: by which sides or faces are these growing Cu nanocrystals connected to form the nanowires? Thermodynamically, crystal planes with lower surface energy are preferably exposed. For an fcc structure, the {111} plane has the lowest surface energy and tends to be exposed on the crystal surface to minimize the total surface energy. However, the presence of large amounts of HDA molecules and Br^- ions could effectively stabilize the {200} planes by selective adsorption on those planes.[9,11] Therefore, as-formed Cu clusters may be inclined to be connected by their active {110} planes, resulting in preferential growth of the nanowires along the ⟨110⟩ direction. This would lead to preferential exposure of the {111} and {200} planes, which is well-consistent with the TEM analysis.

After 5 h of reaction (Figure 3b), it was found that the number of particles was significantly reduced and that significantly increased numbers of nanowires with smoother morphology were present. The nanowires further developed the facet morphology as the reaction time increased to 10 h, indicating a maturing process. Cu particles with cubic and octahedral shapes, which are matured forms of the Cu particles present at early times, were also consistently observed. It is believed that such maturing process is facilitated by the presence of Br^- ions, as Br^- is reported to be a corrosive anion.[12] Such ions may facilitate the migration of Cu atoms from defect or high-energy sites to low-energy sites, leading to the formation of Cu nanowires with perfect structure and morphology. Consistent with the SEM observations, Figure 3d shows the XRD patterns of the nanowires at the different growth steps. Clearly, the (111) and (200) diffractions intensified with increasing reaction time from 2 to 10 h, while the intensity of the (110) peaks decreased. Such observations agree well with the preferential nanowire growth observed by TEM.

dx.doi.org/10.1021/ja3050184 | J. Am. Chem. Soc. 2012, 134, 14283–14286

Moreover, it was also found that CTAB played key roles in the nanowire formation. Figure 4a–d shows SEM images of the

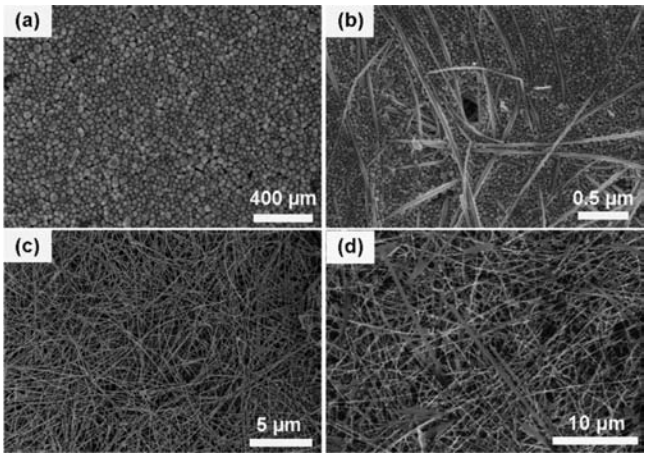

Figure 4. Cu nanowires synthesized in liquid-crystalline media containing a fixed amount of HDA (0.8 g) and different amounts of CTAB: (a) 0.1 g; (b) 0.3 g; (c) 0.5 g; (d) 0.8 g.

reaction products obtained in reaction media containing a fixed amount of HDA (0.8 g) and various amounts of CTAB (0.1, 0.3, 0.5, and 0.8 g, respectively). At low CTAB concentration (0.1 g), only irregular polyhedra were obtained (Figure 4a). Increasing the amount of CTAB to 0.3 g led to the formation of long nanowires accompanied by a large population of irregular polyhedra (Figure 4b). Further increasing the CTAB amount (0.5 g) led to the formation of long nanowires and almost no particles (Figure 4c). Interestingly, continuing to increase the amount of CTAB (0.8 g) resulted in the formation of nanowires and nanoribbons (Figure 4d).

The morphological evolution from irregular polyhedra to nanowires to nanoribbons can be attributed to the varying local molecular environment within this series of reaction media. CTAB, a well-known amphiphilic molecule containing a cationic headgroup and an alkyl chain, can self-organize into various supermolecular structures, such as spherical micelles, hexagonal rods, and liquid-crystalline phases.[13] HDA is also an amphiphilic molecule containing a polar amine group and a nonpolar alkyl chain that can form various liquid-crystalline phases. In their melt mixtures, these alkyl groups tend to form a continuous oil phase, while the cationic groups and the amine moieties may tend to form the counterphase. Similar to other amphiphilic systems, such mixtures may exhibit assembling structures that vary systematically from micellar structures to rods to liquid-crystalline phases depending on the composition. In fact, the mixture containing 0.5 g of CTAB showed XRD diffraction peaks at $2\theta = 2.3$, 4.0, and 7.0° at 180 °C (Figure S1 in the Supporting Information), confirming the formation of tubular liquid-crystalline structures within the reaction medium.[14]

On the basis of the above observations, a formation mechanism can be proposed (Scheme 1). First, the melted CTAB and HDA mixtures provide a medium with a tubular liquid-crystalline structure. Upon the addition of $Cu(acac)_2$, these precursor molecules rapidly coordinate with Br^- and HDA, as indicated by a rapid color change from dark green to light yellow. This coordinating process consequently enriches the metal moieties within the tubular channels. Subsequently, HDA reduces the metal moieties, forming metal clusters and building particles within the tubular channels. Because of preferential

Scheme 1. Formation of Cu Nanowires Directed by the Liquid-Crystalline Structure of the Medium

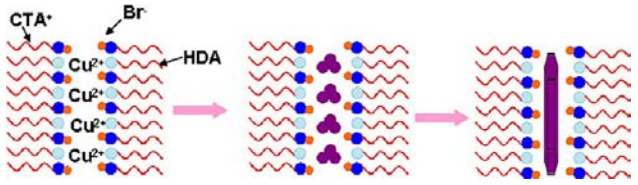

adsorption of HDA and Br^- on the {200} planes, confined growth of the building clusters and particles leads to the formation of Cu nanowires along the ⟨110⟩ direction with preferential exposure of the {111} and {200} planes. Varying the ratio of HDA and CTAB in the reaction medium systematically shifts their assembled structure from micelles to rods to more complicated liquid-crystalline structure (e.g., hexagonal and lamellar phases), accordingly leading to the formation of Cu nanoparticles, nanowires, and nanoribbons with increasing CTAB content.

It is important to mention that without the presence of the catalyst, we did not observe any particles or nanowires even after 10 h. However, upon addition of a piece of Si wafer sputtered with a thin layer of Pt to the reaction medium, nanowires formed rapidly. It should be noted that catalytic reduction of Cu and other metallic moieties is often observed in the electrodeless plating process, where Pt or Pd is commonly used as the catalyst.[15] We believe that the phenomena observed here also arise from the catalytic effect of the Pt thin film. The presence of Pt surface first catalyzes the reduction of Cu ions into metallic clusters or particles, which then migrate to the solution and act as seeds for growth of the nanowires. Indeed, it was found that the reaction solutions turned red after reacting for 30 min, confirming the formation of Cu clusters and their migration to the solution. This seeding mechanism is similar to those reported previously.[16,17]

The capability to synthesize such high-quality nanowires offers ideal building blocks for transparent electrodes. Figure 5a,b shows SEM images of such electrodes with transmittances (T) of 91% and 84.5%, respectively, revealing the formation of continuous nanowire networks. Figure 5c further compares the sheet resistances (R_s) and transmittances of such electrodes with those from the literature (electrodes made from Ag nanowires,[4] CNTs,[5] and Cu nanowires[18]). Clearly, the electrodes constructed from ultralong Cu nanowires exhibited outstanding performance. At $T = 90\%$, they exhibited $R_s \approx 90\ \Omega/\square$, which is significantly lower than that of the Cu nanowire electrode reported by Wiley[18] (~186 Ω/□). These electrodes meet the criteria of high-performance solution-based transparent conductors, which are usually defined as $T \geq 90\%$ and $R_s \leq 100\ \Omega/\square$. Compared with the Ag nanowire electrode previously reported by Hu,[4] the ultralong Cu nanowire electrodes exhibited comparable or even better performance. At $T = 85\%$, the ultralong Cu nanowire electrode exhibited a sheet resistance of ~35 Ω/□, which is comparable to or even lower than that of Ag nanowire electrodes used in organic solar cells[19] or OLEDs.[20] Figure 5d further shows a transmittance plot of such an electrode, demonstrating near-constant transmittance over the visible range.

As proposed by De and Coleman,[21] solution-processed nanowire electrodes generally exhibit a percolative to bulklike transition in conductivity with increasing electrode thickness. The minimum thickness at which a percolative nanowire

dx.doi.org/10.1021/ja3050184 | J. Am. Chem. Soc. 2012, 134, 14283–14286

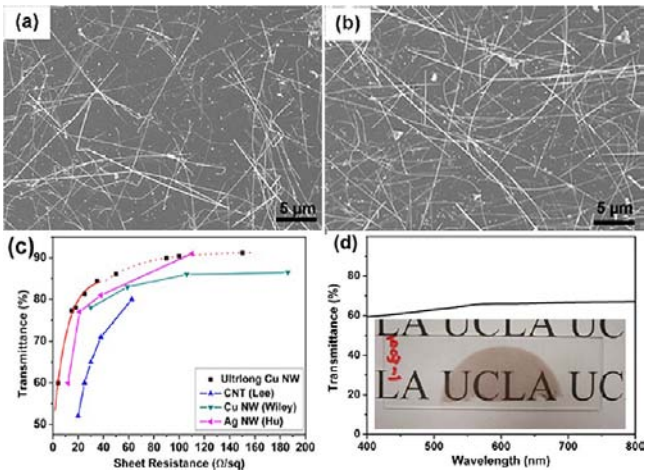

Figure 5. SEM images of Cu nanowire electrodes with (a) 91% and (b) 84.5% transmittance. (c) Comparison of the sheet resistances and transmittances of the electrodes made from the ultralong Cu nanowires with literature values for electrodes made from Cu nanowires (Wiley[18]), CNTs (Lee[5]), and Ag nanowires (Hu[4]). (d) Photograph and corresponding plot of transmittance vs wavelength for an ultralong Cu nanowire electrode (sheet resistance ~5 Ω/□) showing high transparency.

network can be formed is proportional to $T_{tran}^{-1/2}$, where T_{tran} is the transmittance where the transition occurs. It was found that such ultralong Cu nanowire electrodes exhibit a transition at $T \approx$ 81%, while the reported Cu nanowire electrodes showed a transition at significantly lower transmittance (~60%).[1] The lower percolative thickness observed can be attributed to the long length and excellent dispersibility of the nanowires, which enables the construction of effective conductive networks using smaller amounts of nanowire. For such electrodes, the figure of merit, a performance parameter that is generally defined as the ratio of the electrical conductivity to the optical conductivity, was estimated as 93, which is significantly higher than those of the reported Cu nanowire electrodes (52),[1] CNT electrodes (1.5), and graphene electrodes (0.25),[21] confirming the high performance of the obtained electrodes.

We recognized that the stability of Cu nanowire thin films can be problematic for device application. Nevertheless, it was found that the stability of such nanowire films is dependent on thickness. For example, thin films (~100 Ω/□) exhibited a rapid increase in sheet resistance within hours, while thick films (~10 Ω/□) exhibited almost constant sheet resistance even after 10 days of exposure to ambient conditions (Figure S2). It was also found that coating the nanowire films with polymers or treating them with ambient-pressure hydrogen plasmas afforded highly conductive electrodes with excellent stability. This will be the subject of a future report.

In conclusion, we have demonstrated the synthesis of ultralong Cu nanowires with excellent dispersibility. This method should be further extended to the fabrication of other metal nanowires, providing excellent building blocks for the construction of transparent electrodes for flexible displays, photovoltaics, and other applications. Further studies in device integration are underway.

■ ASSOCIATED CONTENT

Ⓢ Supporting Information

Detailed synthesis procedure for Cu nanowires, preparation of Cu nanowire thin films, and XRD patterns of HDA/CTAB mixtures. This material is available free of charge via the Internet at http://pubs.acs.org.

■ AUTHOR INFORMATION

Corresponding Author

jingsun@mail.sic.ac.cn; hexing-li@shnu.edu.cn; luucla@ucla.edu

Author Contributions

⊥D.Z. and R.W. contributed equally.

Notes

The authors declare no competing financial interest.

■ ACKNOWLEDGMENTS

This work was financially supported by the Center for Molecularly Assembled Material Architectures for Solar Energy Production, Storage and Carbon Capture, an Energy Frontier Research Center funded by the U.S. Department of Energy, Office of Science.

■ REFERENCES

(1) Rathmell, A. R.; Bergin, S. M.; Hua, Y. L.; Li, Z. Y.; Wiley, B. J. *Adv. Mater.* **2010**, *22*, 3558.
(2) Wang, R. R.; Sun, J.; Gao, L. A.; Zhang, J. *ACS Nano* **2010**, *4*, 4890.
(3) Wang, R. R.; Sun, J.; Gao, L. A.; Xu, C. H.; Zhang, J.; Liu, Y. Q. *Nanoscale* **2011**, *3*, 904.
(4) Hu, L.; Kim, H. S.; Lee, J. Y.; Peumans, P.; Cui, Y. *ACS Nano* **2010**, *4*, 2955.
(5) Kim, U. J.; Lee, I. H.; Bae, J. J.; Lee, S.; Han, G. H.; Chae, S. J.; Gunes, F.; Choi, J. H.; Baik, C. W.; Kim, S. I.; Kim, J. M.; Lee, Y. H. *Adv. Mater.* **2011**, *23*, 3809.
(6) Yu, Z. B.; Zhang, Q. W.; Li, L.; Chen, Q.; Niu, X. F.; Liu, J.; Pei, Q. B. *Adv. Mater.* **2011**, *23*, 664.
(7) Wu, H.; Hu, L. B.; Rowell, M. W.; Kong, D. S.; Cha, J. J.; McDonough, J. R.; Zhu, J.; Yang, Y. A.; McGehee, M. D.; Cui, Y. *Nano Lett.* **2010**, *10*, 4242.
(8) Dan, B.; Irvin, G. C.; Pasquali, M. *ACS Nano* **2009**, *3*, 835.
(9) Jin, M. S.; He, G. N.; Zhang, H.; Zeng, J.; Xie, Z. X.; Xia, Y. N. *Angew. Chem., Int. Ed.* **2011**, *50*, 1.
(10) Ouardi, S.; Fecher, G. H.; Felser, C.; Blum, C. G. F.; Bombor, D.; Hess, C.; Wurmehl, S.; Büchner, B.; Ikenaga, E. *Appl. Phys. Lett.* **2011**, *99*, No. 152112.
(11) Xia, Y. N.; Xiong, Y. J.; Lim, B.; Skrabalak, S. E. *Angew. Chem., Int. Ed.* **2009**, *48*, 60.
(12) Wiley, B. J.; Chen, Y. C.; McLellan, J. M.; Xiong, Y. J.; Li, Z. Y.; Ginger, D.; Xia, Y. N. *Nano Lett.* **2007**, *7*, 1032.
(13) Li, H.; Zhang, Y.; Liu, H. F.; Wang, J. *J. Am. Ceram. Soc.* **2011**, *94*, 3267.
(14) Xu, J.; Luan, Z. H.; He, H. Y.; Zhou, W. Z.; Kevan, L. *Chem. Mater.* **1998**, *10*, 3690.
(15) Mills, A.; Meadows, G. *Inorg. Chem.* **1993**, *32*, 3433.
(16) Azulai, D.; Belenkova, T.; Gilon, H.; Barkay, Z.; Markovich, G. *Nano Lett.* **2009**, *9*, 4246.
(17) Taub, N.; Krichevski, O.; Markovich, G. *J. Phys. Chem. B* **2003**, *107*, 11579.
(18) Rathmell, A. R.; Wiley, B. J. *Adv. Mater.* **2011**, *23*, 4798.
(19) Zhu, R.; Chung, C. H.; Cha, K. C.; Yang, W. B.; Zheng, Y. B.; Zhou, H. P.; Song, T. B.; Chen, C. C.; Weiss, P. S.; Li, G.; Yang, Y. *ACS Nano* **2011**, *5*, 9877.
(20) Li, L.; Yu, Z. B.; Hu, W. L.; Chang, C. H.; Chen, Q.; Pei, Q. B. *Adv. Mater.* **2011**, *23*, 5563.
(21) De, S.; Coleman, J. N. *MRS Bull.* **2011**, *36*, 774.